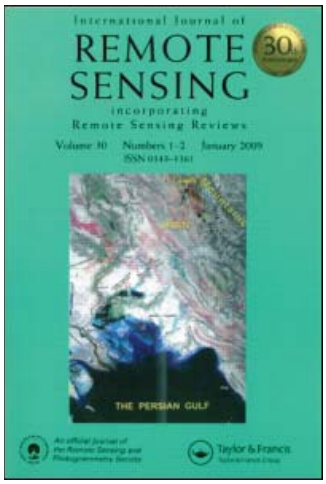

International Journal of Remote Sensing

Publication details, including instructions for authors and subscription information:
http://www.informaworld.com/smpp/title~content=t713722504

Contrail observations over Southern and Eastern Asia in NOAA/AVHRR data and comparisons to contrail simulations in a GCM

R. Meyer[a]; R. Buell[b]; C. Leiter[c]; H. Mannstein[b]; S. Pechtl[bd]; T. Oki[e]; P. Wendling[a]

[a] SunTechnics GmbH, D-20537 Hamburg, Germany [b] DLR - Oberpfaffenhofen, Institut für Physik der Atmosphäre, D-82234 Wessling, Germany [c] Science and Computing AG, München, Germany [d] now at Institute for Environmental Physics, University of Heidelberg, D-69120 Heidelberg, Germany [e] Institute of Industrial Science, University of Tokyo, Tokyo 153-8505, Japan

To cite this Article Meyer, R. , Buell, R. , Leiter, C. , Mannstein, H. , Pechtl, S. , Oki, T. and Wendling, P.(2007) 'Contrail observations over Southern and Eastern Asia in NOAA/AVHRR data and comparisons to contrail simulations in a GCM', International Journal of Remote Sensing, 28: 9, 2049 — 2069

To link to this Article: DOI: 10.1080/01431160600641707

URL: http://dx.doi.org/10.1080/01431160600641707

International Journal of Remote Sensing
Vol. 28, No. 9, 10 May 2007, 2049–2069

Contrail observations over Southern and Eastern Asia in NOAA/AVHRR data and comparisons to contrail simulations in a GCM

R. MEYER†, R. BUELL‡, C. LEITER§, H. MANNSTEIN*‡, S. PECHTL‡¶, T. OKI‖ and P. WENDLING†

†SunTechnics GmbH, Anckelmannsplatz 1, D-20537 Hamburg, Germany
‡DLR – Oberpfaffenhofen, Institut für Physik der Atmosphäre, D-82234 Wessling, Germany
§Science and Computing AG, München, Germany
¶now at Institute for Environmental Physics, University of Heidelberg, D-69120 Heidelberg, Germany
‖Institute of Industrial Science, University of Tokyo, Tokyo 153-8505, Japan

For the first time the contrail cover for a region covering Thailand and surrounding regions as well as for the region of Japan and its surroundings are determined by remote sensing observations. Locally received NOAA/AVHRR satellite data are analysed by a fully automated contrail detection algorithm. For both regions approx. 400 NOAA-14 satellite scenes from four months of the year 1998 were analysed. Both regions show sufficient air traffic to produce an observable amount of contrails. Thus we are able to measure for the first time contrail frequencies in the tropics and compare it to a nearby mid latitudinal region. The annual average of the daily mean contrail cloud coverage is 0.13% for the Thailand region and about 0.25% for the Japan region. For both regions the contrail cover is largest during spring. The daily cycle shows surprisingly high contrail coverage during night in spite of lower air traffic densities during night time. The satellite observed contrail cover is compared with simulations of contrails by use of the general circulation model ECHAM4 related to air traffic emissions of 1992. While the derived patterns of the regional contrail distributions agree well, the contrail coverage derived from satellite data is larger than the simulated coverage. This discrepancy appears to be mainly due to an increase in air traffic in the time period between the model study and the observations.

1. Introduction

There is growing concern that the emissions by increasing air traffic may change the atmospheric composition and, as a consequence, also climate (IPCC 1999). Air traffic influences the atmosphere through the emission of various gases and particles. Among these, water vapour and aerosol particles acting as cloud nuclei are of special interest because they support cloud formation and by that modify an important climate factor. Clouds may be formed in the wake of aircraft in the form of line shaped clouds (condensation trails, contrails) when the exhaust gases mix with cold ambient air and reach or exceed liquid saturation. By that liquid droplets form on cloud condensation nuclei and below temperatures of about -40°C

*Corresponding author. Email: Hermann.Mannstein@dlr.de

International Journal of Remote Sensing
ISSN 0143-1161 print/ISSN 1366-5901 online
http://www.tandf.co.uk/journals
DOI: 10.1080/01431160600641707

immediately start to freeze and form cirrus-like clouds. For given atmospheric temperature and humidity conditions contrail formation can be accurately predicted according to the modified Schmidt-Appleman criterion (Schumann 1996). Persistent contrail formation requires an ice-saturated ambient atmosphere (Jensen *et al.* 1998). The cirrus clouds induced by air traffic are formed obviously where no natural clouds would have formed otherwise.

Generally, contrails will cause a heating of the troposphere. According to Strauss *et al.* (1997), who used a 1-D radiative convective model to simulate the climatic conditions of Central Europe, the mean surface temperature will increase by about 0.05 K for a 0.5% increase of current ice cloud cover. By use of a 2-D radiative convective model Liou *et al.* (1990) obtained a 1 K increase in surface temperature over most of the northern latitudes for an assumed additional cirrus cloud cover of 5%. The potential effects of contrails on global climate were firstly simulated by Ponater *et al.* (1996) using a general circulation model and by introducing an additional cirrus cloud cover in the regions with large air traffic. The increase in surface temperature was only statistically significant for an assumed 5% additional cirrus cloud cover in the main traffic region. For this value the surface temperature increased by about 1 K within the North Atlantic flight corridor.

In order to accurately determine the effects of contrails on climate regional and global observations of contrail cloudiness are necessary. However, observations of air traffic related additional high cloudiness have been obtained up to now for only a few selected regions. Bakan *et al.* (1994) derived by visual inspection of AVHRR data for 1979–1981 and 1989–1992 a mean day-time contrail cover of 0.5% for the eastern North Atlantic region and north-western part of Europe. A maximum coverage of 2% occurred centred along the North Atlantic air traffic routes during summer. On the other hand, Mannstein *et al.* (1999) developed an automated pattern recognition technique for AVHRR data to differentiate line-shaped high clouds from fuzzy cirrus clouds based on data of the 11 μm and 12 μm- channels. By use of this method Meyer *et al.* (2002) analysed the contrail cover over central Europe for a two year period starting in March 1995 using passages of the NOAA-14 satellite. According to the results contrail frequency peaks around February/March and has a minimum during July/August. In the annual mean, line-shaped contrails at noon cover about 0.5% of the area over central Europe.

Contrail formation potential and contrail cover were estimated on the global scale using meteorological analysis data for temperature and humidity (ECMWF reanalysis data, Sausen *et al.* 1998), applying the modified Schmidt-Appleman criterion and a suitable function between fuel consumption and additional cloud cover. The obtained cloud cover is then scaled to the observed value of 0.5% over Europe and the eastern Atlantic according to Bakan *et al.* (1994). Based on the fuel consumption of 1992 the computed contrail cloud cover reaches 0.1% in the global mean with a local maximum of 5% over the eastern United States of America. The computed contrail coverage over south-eastern Asia is smaller than over Europe and North America but still noticeable high. Due to the high frequency of ice saturated air masses in the south-east Asia region, relatively high contrail coverage can be expected.

Recently, a similar scheme to diagnose globally the properties of contrails was applied within the framework of the general circulation model ECHAM4 (Ponater *et al.* 2002). Again, the regional contrail coverage was calibrated to an annual mean value of 0.5% over the Eastern Atlantic and Western Europe. In figure 1 we show

results for global contrail coverage derived according to Ponater *et al.* (2002) obtained by an improved calibration method that takes into account day/night differences observed by Bakan *et al.* (1994) and the daily cycle of air traffic. For the optically visible contrails a global average cloud coverage of 0.06% is calculated. For the region covering the Asian flight corridor extending from Indonesia to Japan the obtained contrail cloud cover amounts to 0.17% for Japan (blue box, figure 1) and to 0.06% for Thailand (green box, figure 1).

Until now, no contrail observations are available for the region of the Asian flight corridor. This is important to check further the above mentioned global model. Only when the model is validated in different areas of the world it can be reliably used for further diagnosis of contrail induced cloudiness and for the prediction of the related global and regional climate change. In addition, contrail observations are needed in the Asian region also in view of the rapidly increasing air traffic in this area. According to the IPCC report (1999) the global mean of the total radiative forcing due to aircraft emissions will grow from a present value of 0.05 W/m^2 to 0.19 W/m^2 in 2050. This is derived from a reference scenario for 1992 with a 7-fold increase in air traffic and a 3-fold increase in fuel consumption in the time period from 1992 to 2050. Although the expected globally averaged radiative forcing seems to be low compared to the forcing due to the increase in greenhouse gases the regional effects of contrail induced cloudiness may be much larger.

Up to now all global contrail simulations (Sausen *et al.* 1998, Ponater *et al.* 2002) are scaled to the observations of Bakan *et al.* (1994) in the Europe and Eastern North Atlantic region. Further, these results on global contrail cloudiness are the

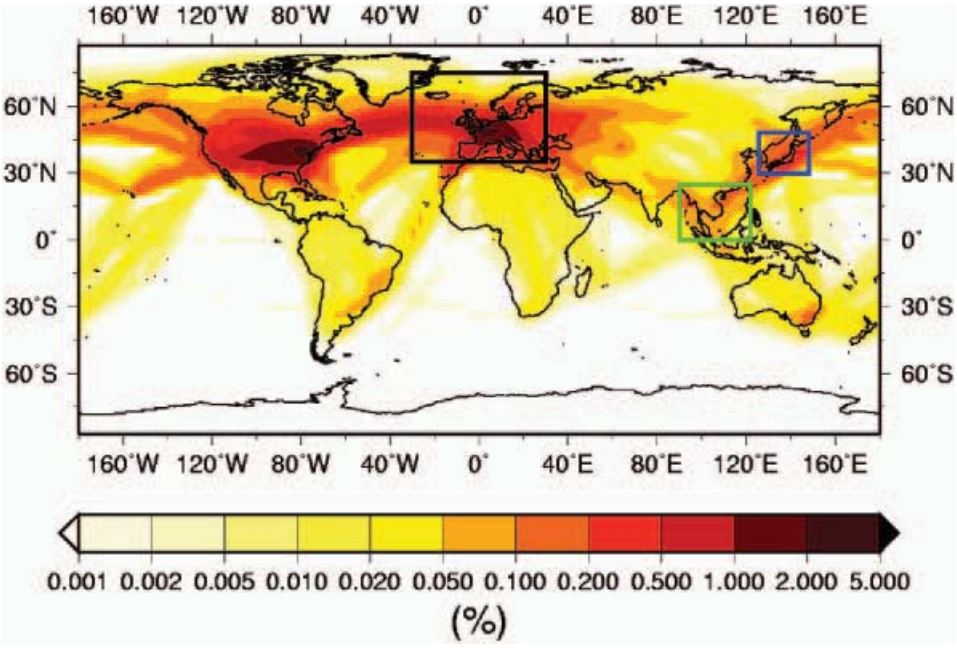

Figure 1. Global coverage by contrails from simulations with the GCM ECHAM4 (after Ponater *et al.* (2002) using a revised calibration method as explained in §4.1). The black rectangle shows the region used for calibration of the GCM by the results of Bakan *et al.* (1994). The two regions observed in this work by AVHRR satellite data are indicated in green ('Thailand region') and blue ('Japan region').

basis for the forecasts on future effects (Gierens *et al.* 1998) and contrails' impact on radiative forcing (Minnis *et al.* 1999). The IPCC contrail assessment in 'Aviation and the global atmosphere' (1999) is mainly based on these results. However, from more recent studies of Ponater *et al.* (2002), Marquart and Mayer (2002), and Meyer *et al.* (2002) we learn that uncertainties of the contrail radiative forcing seem to be even larger than estimated in the IPCC (1999) report.

Therefore independent checks of contrail properties are urgently needed. Preferably this task is carried out in an area far away from the calibration area where air traffic is high enough to produce a notable amount of contrails. The present paper aims to report observations of the contrail cover using NOAA/AVHRR satellite data for the regions surrounding Japan and Thailand. The Southern and Eastern Asian region represents an area where the largest growth rates for air traffic are expected.

The paper will be structured as follows: In §2 the basic method for the detection of contrails and the determination of their cloud cover from NOAA/AVHRR satellite data is described. In §3 the satellite data set is described and the results for the derived contrail cloud cover are presented. In §4 the results are compared to those of the global circulation model ECHAM4. §5 presents further discussions and implications of this comparison. Finally, in §6 the conclusions are given.

2. Deriving contrail coverage from AVHRR imagery

To assess the influence contrails have on climate we need to observe their average properties. Besides contrail area coverage also optical depth, particle size distribution and shape of the ice particles are of interest. Here we focus on contrail coverage which we define as the temporal average of contrail occurrence averaged over a certain area.

To solve this task by observations we need a remote sensing instrument that is able to see most contrails principally and for which large data sets for the envisaged regions are available. Further we want to be able to analyse contrails during daytime and night time with comparable efficiency. To achieve significant results we request a high repetition rate and a spatial resolution that is suitable to detect most contrails. The latter request implies the usage of polar orbiting satellites, like the NOAA-POES series carrying the AVHRR instrument. Unfortunately the swath of a single NOAA satellite near the equator is covered only twice per day. Although more satellites exist, which cover the morning and afternoon hours of the daily cycle, only results from the instrument on-board NOAA-14 are used to achieve comparable results. As explained by Mannstein *et al.* (1999) the algorithm is very sensitive to minor changes of the instrument characteristics. Therefore, a daily cycle derived by use of different instruments could be very misleading.

A high spatial resolution of the instrument is requested as contrails usually are about 200 m wide after formation. Only contrails that do not evaporate within some minutes after formation are relevant for average area cover (Ponater *et al.* 1996). These persistent contrails mostly spread strongly and are able to cover large proportions of the sky. Due to the downdraft in the aircraft wake the geometrical depth of contrails is in the order of 500 m. On the other hand, the horizontal width will be enhanced most effectively by horizontal wind shear. Usually 10 min to 20 min after formation contrail width is in the order of 1 km. Often these contrails and also narrower ones can be clearly recognized in satellite images. The reason is that they usually appear as straight narrow lines. As long as they are thick enough and keep

their artificial looking shape human observers can easily distinguish them from natural clouds or other image features.

For these reasons we use data of the AVHRR instrument which successfully operates on the NOAA polar orbiting platforms since many years. The repetition rate of two overpasses per day at the equator is sufficient. Its thermal infrared channels at 10.2 μm to 11.3 μm (channel 4) and 11.5 μm to 12.5 μm (channel 5) allow day and night observations. The provided spatial resolution of about 1 km is not perfect but allows detecting most persistent contrails.

2.1 *Contrail detection*

For the separation of contrail and contrail-free pixels in AVHRR data we make use of the algorithm developed by Mannstein *et al.* (1999). This contrail detection scheme uses brightness temperature images of channel 4 (T_4) and channel 5 (T_5). Ice clouds can be well recognized in images that show the temperature difference TD of the two channels (T_4–T_5). This effect is strongest for non-opaque ice clouds with small ice particles which are typical for young contrails.

To enable similar detection efficiency under various conditions and to avoid misdetections at coastlines or other linear structures as mountain ridges both images T_5 and T_D are normalised by their local standard deviation. For this normalization we use the standard deviation in the 5×5 pixel surrounding, SDT_5 for T_5 and $SDTD$ for T_D. Both normalized images $N5$ and ND are then combined to the image N. This normalized image N shows contrails as bright lines. This 'ridges' in the image now are selected by convolution with a line detection kernel of 19×19 pixel size applied in 16 different directions. From these intermediate results candidates for contrail pixels are selected by parameters that check radiometric and geometric features typical for contrails. These are $T_D > 0.2$ K, $N > 1.5$ and a gradient condition that further avoids misdetection of coastlines. Geometric checks are a minimum length of the contrail segments, (15 pixels) the requirement, that the correlation of all pixels of a contrail segment must be better than 0.975 to a straight line and a minimum number of pixels. This is fixed to a number of 10 per contrail segment. These parameters were empirically set. The characteristics of the contrail detection algorithm strongly depend on them. Thus, to achieve comparable detection efficiency we fixed all parameters to the values mentioned in Mannstein *et al.* (1999). The chosen parameter setting is adapted to a rather low false alarm rate when applied to NOAA-14/AVHRR data, which are used in this paper.

The contrail detection algorithm is applied to all available scenes in satellite projection. To cover large areas we try to process the full satellite passes. As the contrail detection process makes extensive use of the available computer memory we split up all overpasses with more than 2048 pixels into two parts. These are processed separately and are recombined afterwards. All pixel-based contrail masks then are remapped to a common projection. Here we use a 1 km $\times$ 1 km grid with common reference latitude of 12.5° N for both regions.

2.2 *Contrail coverage*

The algorithm pointed out the above results in simple binary decisions on contrail or no contrail occurrence for each pixel. Partly contrail filled pixels either get classified as 'fully contrail covered' or 'not contrail covered'. Thus, actual contrail coverage may only be given as a box average or by temporal averaging. This temporal

averaging separately is applied for day and night-time NOAA-overpasses to allow for comparison of day and night contrail coverage. For this the 'local contrail frequency' is calculated from the total number of contrails detected at a certain geographical location divided by the total number of satellite observations at this location.

Of course, results on contrail coverage are much more reliable, if a large amount of data is taken into account. Meyer *et al.* (2002) conclude from Poisson statistics that more than 1000 measurements per pixel are needed to get significant results, if the event 'contrail occurs' has a probability of 0.2%. As we expect a maximum number of measurements in the order of 200 per time of day, we have to combine both types of averaging to enhance significance. First we stack as many satellite scenes as possible for the requested analysis period, e.g. all night time data for January. From this we calculate the local frequency and then average spatially.

The spatial averaging may be either a simple box average or can be done in a more refined way. For the cloud cover maps shown here we will apply the spatial filtering as proposed by Meyer *et al.* (2002). This filter basically is a circular kernel with an extension of 120 km × 120 km and a weighting function similar to a Gauss curve. When applying this filter to maps with 1 km × 1 km resolution the averaging effect is equal to averaging over 3604 km^2. Thus, by this procedure it is possible to derive local contrail coverage from single binary contrail decision images. This is true for the actual coverage during a satellite pass, but a single scene is not at all representative for the long-term average situation for contrails. To obtain statistically significant averages of contrail cloud cover independent probing is required. The data set should have a good representation of weather situations typical for the region of interest. According to Meyer *et al.* (2002) the minimum number of days to derive meaningful results by this method is 16. To achieve reliability better than 50% a total of 64 measurements are recommended.

As already noticed by Mannstein *et al.* (1999) the contrail detection is influenced by the heterogeneity of the background. The detection efficiency of the applied algorithm is higher in homogeneous parts of the brightness temperature image than in parts where great variations occur. In cloud free situations homogeneous areas are found over the sea or over flat land. Examples for heterogeneous situations are mountain or coast regions. In cloudy situations contrails are, for example, easier to detect above stratus cloud layers than above broken cumulus cloud fields.

Mannstein *et al.* (1999) found that the long-term average of the standard deviation in the 12 μm channel SDT_5 is anti-correlated to the contrail occurrence and therefore SDT_5 is a good measure to indicate the average detectability of contrails. Here we apply the same type of 'heterogeneity-correction' as originally developed from the Europe data set. The corrected contrail coverage N_{ct} is derived according to

$$N_{ct} = 1/(1 - 0.397/(0.489 \times SDT5)) \times N_{ct}^{'} \tag{1}$$

where N_{ct}' is the uncorrected contrail coverage. To avoid instabilities at this correction step SDT_5 should be averaged over a very long period for each time of day.

In Meyer *et al.* (2002) a more advanced post-processing procedure is described. Additionally to the correction of variable detection efficiency this new method treats the false alarm rate which also depends on the background homogeneity. Applied to data from Europe the new post-processing leads to a more realistic best estimate on

contrail coverage, while the post-processing of Mannstein *et al.* (1999) results in a lower estimate. For Europe this lower estimate for contrail coverage is approximately 33% below the best estimate of Meyer *et al.* (2002). Unfortunately, the method of Meyer *et al.* (2002) could not be applied here. It was found that the false alarm correction works only properly for regions that have high average contrail coverage. The procedure severely underestimates contrail coverage for regions and times where uncorrected contrail cover is in the order of the estimated false alarm rate.

Further, from the data for the Thailand region it was deduced that the false alarm correction needs to be adapted to tropical meteorological conditions. By visual inspection of some scenes from the Thailand data set it was found that in this region almost no false alarms happen. Thin cirrus streaks that cause 90% of the false alarms in midlatitudes (Meyer *et al.* 2002) are very seldom in the tropical climate. The development of an adapted false alarm correction would have needed a much larger data set than available for our investigation. To allow direct comparison of the two regions, we use post-processing by Mannstein *et al.* (1999) for both regions. This procedure neglects the low detection efficiency of the algorithm when using NOAA-14 data. Thus we must be aware that the derived corrected contrail coverage $N_{ct.min}$ represents a lower estimate.

3. Results

3.1 *Data availability and observing conditions*

The method described above needs AVHRR data in the highest possible resolution of approximately 1 km × 1 km which is available via direct broadcast from satellite in the HRPT-form (high resolution picture transmission). For the regions of interest we got access to HRPT-data received at the University of Tokyo for the Japan region and at the Asian Institute for Technology in Bangkok for the Thailand region. From both institutions we received approximately 400 AVHRR scenes for the year 1998. To get an impression on annual variability the mid-season months (January, April, July and October) were requested. For the Japan region due to availability April data has to be exchanged against March data. Each of these scenes covers a region of approximately 3000 km × 5000 km. Two daily overpasses with highest satellite elevation angle were selected: one for daytime and one for night time. For processing reasons the satellite scenes often had to be separated into two parts. As may be seen in figure 2 the reunification of the separately processed parts sometimes failed, which results in poor coverage of the southern parts of the Japan region especially during night.

The nadir tracks move towards the west from day to day which results in a variable number of measurements for each investigated point (see figure 2). In these maps we can also see that the direction of the track is towards NNW for the ascending daytime satellite passes and towards SSW for the descending daytime satellite passes. Thus, poorest data coverage is in the corners of these maps farthest from the satellite receiving station.

The two regions displayed in figure 2 show some overlap. Originally, it was planned to compare the results there, but had to be abandoned as the number of measurements is insufficient in both areas to derive reasonable results. According to Meyer *et al.* (2002) the applied contrail coverage processing requires at least 16 measurements to report significant results when averaging boxes as large as

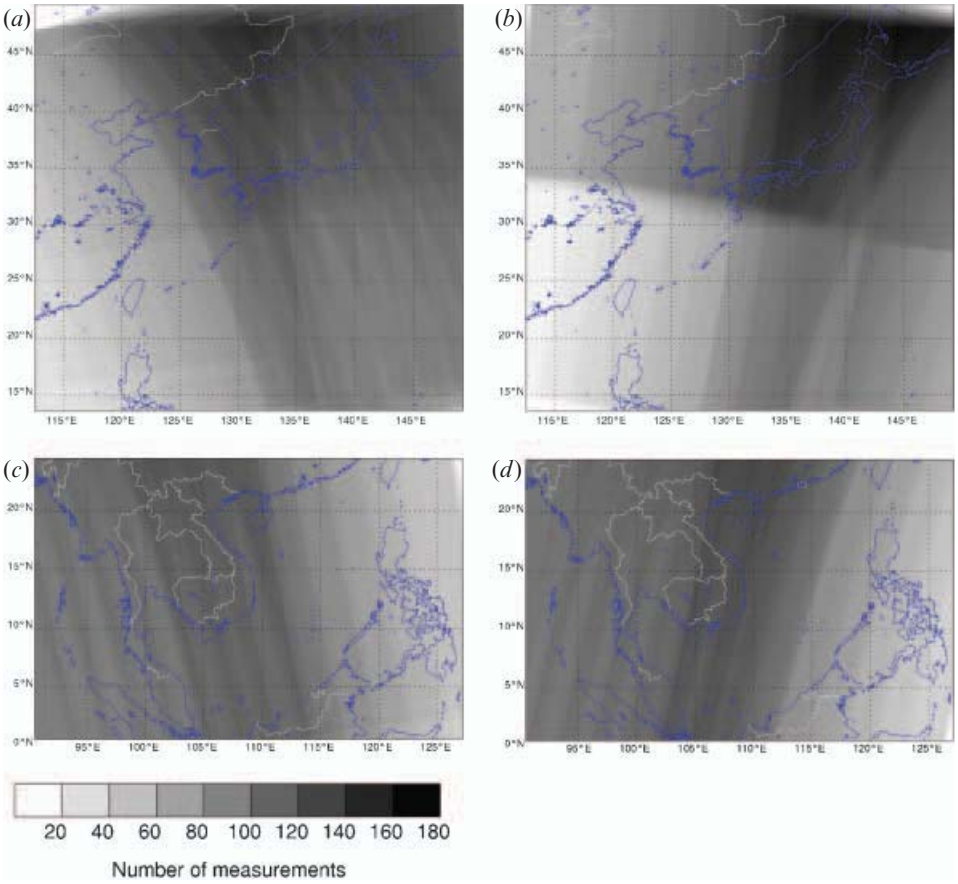

Figure 2. Total number of measurements in both observing regions (Japan region in maps (*a*) and (*b*), Thailand region in maps (*c*) and (*d*), left ((*a*) and (*c*)) for daytime and right ((*b*) and (*d*)) for nighttime). For the maps of average contrail coverage in figure 4 and 5 a minimum of 64 observations is needed to obtain significant results. For the comparison to ECHAM4 GCM results with a resolution of approximately $3.75^\circ \times 3.75^\circ$ (T30) a minimum number of 16 observations per box is needed.

$3.75^\circ \times 3.75^\circ$. This is the size of the model boxes we use later on for inter-comparison. To show contrail coverage results in a smoothed satellite resolution the minimum number of measurements needed is 64. By this condition the Japan region is largely cut from the longitudinal margins 115° E and 149.8° E down to 125.625° E and 148.125° E. Latitudinal margins are reduced even stronger from 15° N up to 29.689° N and from 50° N down to 48.245° N. The Thailand region shrinks less: Only the eastern margin is reduced from 127.689° E to 121.875° E.

As also mentioned in §2.2 the thermal homogeneity of the background influences the quality of the derived contrail coverage. Figure 3 displays maps of the annual average of the standard deviation SDT_5 separately for night and day. These maps indicate that detectability of contrails is best during night time. Differences between land and sea are small. Only in the Japan region mainly the Chinese coast shows high SDT_5-values during night. Heating of land during the day leads to high thermal heterogeneity. It is strongest in subtropical regions and exceedingly high in mountainous regions where temperature contrasts of shaded and illuminated slopes

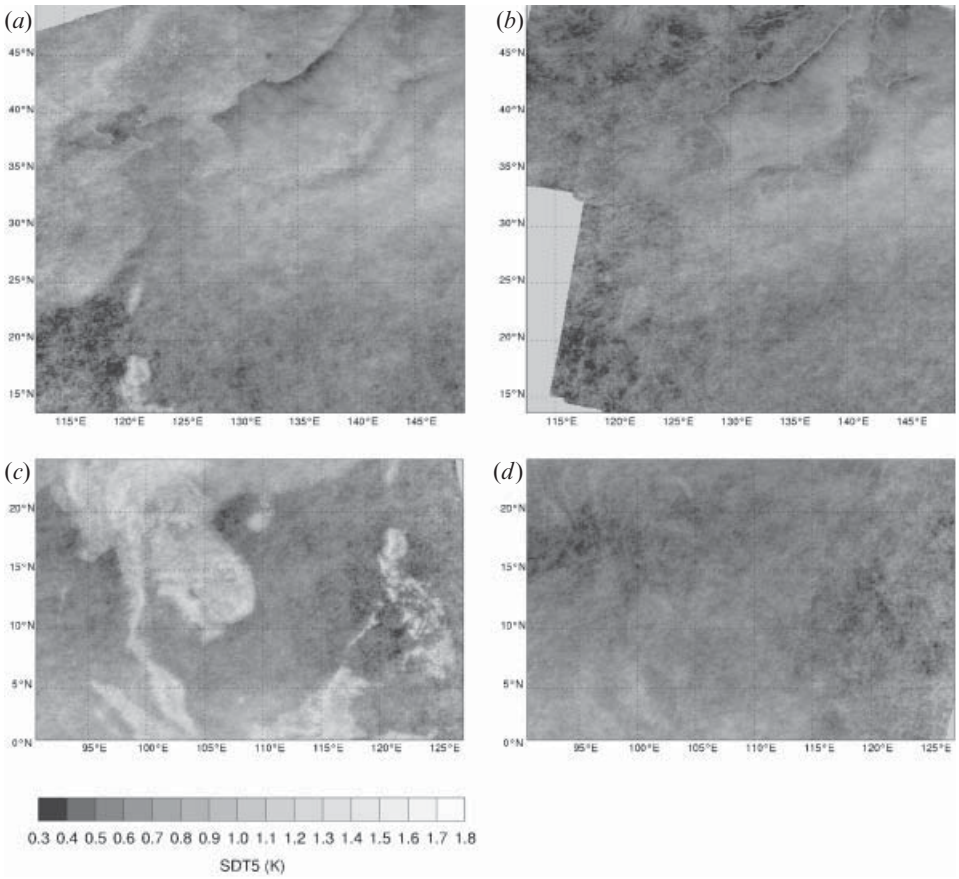

Figure 3. Average standard deviation in 5×5 pixel surrounding of channel 5 (SDT_5). These images show the background heterogeneity, which affects detectability of contrails. For $SDT_5 > 1.1$ K no results on contrail coverage are derived. The figures on the right for night time show that temperature contrasts are much less during night. Due to less surface heat during night the observability for contrails in the used IR channels is much better than during daytime. Areas with less than 16 measurements are blanked to avoid insignificant maxima greater 1.8 K.

are very high at the 5 km scale. In the tropics we recognize that SDT_5 is also very high but compared to the subtropics it is more diluted. Reason is that in the tropics more clouds contribute to the high SDT_5. Of course, the position of clouds is variable from day to day which results in a smoothing effect when averaging many days. Another reason could be a higher frequency of thin transparent clouds which also smoothes surface temperature contrasts.

Meyer *et al.* (2002) found that due to the normalization process the current detection algorithm does not produce reasonable results for regions where SDT_5 exceeds 1.1 K. Thus we exclude these areas from the maps and do not regard them in our statistics.

The SDT_5-arrays are used to homogenize the contrail cover according to (1). This processing step leads to comparable results over land and sea. To make day and night results comparable as well we use separate night and day SDT_5-values. To avoid locally overstated correction effects a smoothed SDT_5-mask is applied.

According to Meyer *et al.* (2002) SDT_5 is convoluted by a 60 km × 60 km low-pass filter kernel that is adapted to the typical surrounding sphere that may influence the quality of the detection algorithm.

3.2 *Detected contrails*

All results of the contrail decision masks according to Mannstein *et al.* (1999) are remapped scene by scene to a common projection for both regions under investigation. These remapped masks are stacked to monthly sums and further to the annual sum consisting of four midseason months. These stacked maps are displayed in figure 4. They show the absolute number of contrails detected per pixel in the 1 km × 1 km resolution-and give a first impression on the contrail distribution in the two regions of interest. The stacked maps help to check the data for outliers. Frequent misdetections of stationary features would show up. Fortunately, we do not recognize any suspicious structures in any of the four maps of figure 4.

3.3 *Observed contrail coverage*

Finally, we derive the contrail coverage as described shortly in §2.2 according to Mannstein *et al.* (1999). The results shown in figures 5 and 6 represent a lower estimate of contrail coverage. The detection algorithm mostly detects contrails that can be clearly distinguished from natural clouds. The detection scheme does hardly detect contrails that are optically very thin (visible optical depth below 0.05), contrail segments that are very short (shorter than 15 km) or sharply bent. We do not expect great climatic impact of losing those. Unfortunately, the algorithm also is not able to detect widespread fuzzy contrails which look very similar to natural cirrus and therefore are hard to distinguish. The coverage of these additional contrail induced cirrus clouds could be an order of magnitude higher (Liou *et al.* 1990, Schumann 2002). Nevertheless the given results on contrail coverage represent a good estimate for the lower border. Due to the applied normalization and because of the correction of the variable detection efficiency different regions and times of day can be well compared.

In both analysed regions we recognise that large areas are almost free of contrails. We can see that contrail coverage often clusters mainly in linear structures along the major international traffic routes. The length of these contrail patterns is typically in the order of some 100 km, their width is in the range from 50 km to 100 km. Along these traffic routes the annual average coverage is in the range from 0.4% to 0.8%. Peaks of more than 1% average coverage are reached where major routes cross. The maximum of almost 2% is reached during day and night south of Taiwan and also during daytime in the Tokyo area. Huge airports usually cannot be recognised in our maps of contrail cover because starting and landing air-planes do not form contrails. Under typical atmospheric conditions air-planes need to fly at heights of at least 7 km to form contrails. Thus, we assume that there must be a major crossing of air routes in the Tokyo UIR (upper flight information region).

The day and night averages over the whole displayed area are 0.25% for the Japan region and 0.13% for the Thailand region. Mannstein *et al.* (1999) report 0.3% (lower estimate) and Meyer *et al.* (2002) 0.5% (best estimate) for the average contrail coverage over Europe. This means that contrail activity in the Japan area is almost

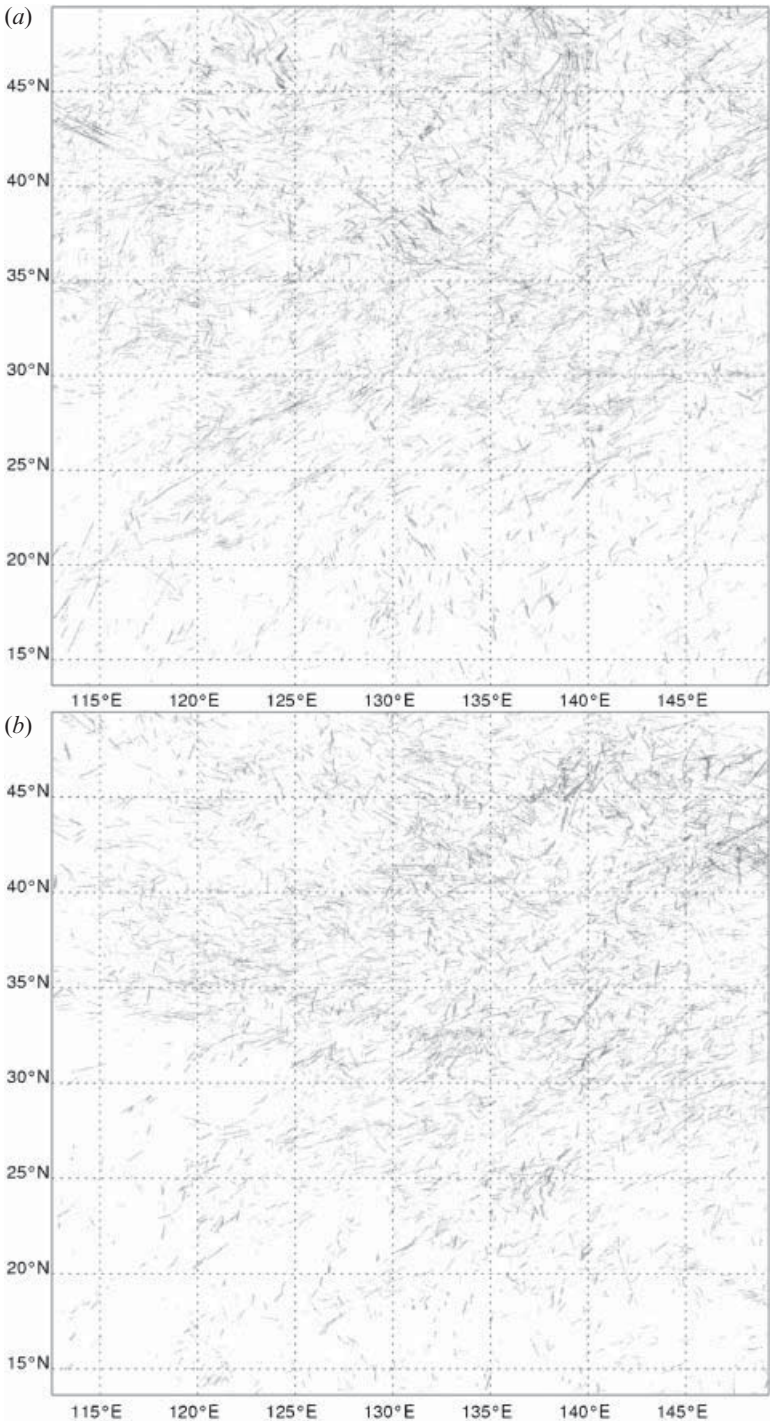

Figure 4. Contrails detected in Japan region for 1998 (map (*a*): day-time, map (*b*): night-time).

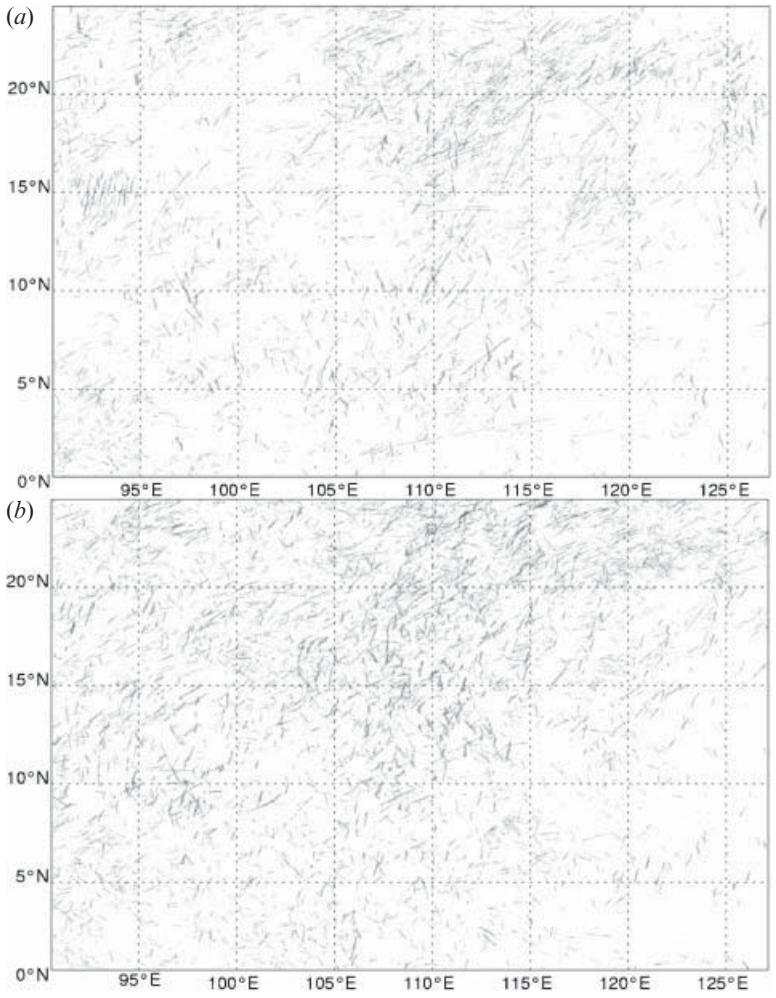

Figure 5. Contrails detected in Thailand region for 1998 (map (*a*): day-time, map (*b*): night-time).

as strong as over Europe but over the Thailand region obviously less contrails occur than over Europe.

Day- and night time coverage of the full displayed map are 0.27% and 0.22% for the Japan region and 0.13% and 0.14% for the Thailand region. Thus, there seems to be a very small daily cycle of contrail coverage assuming that the two inspected time slots are representative for the daily cycle. These small day/night differences for the Asian regions are a surprising result as Meyer *et al.* (2002) found a day/night-ratio of factor three for Europe.

4. Comparison of observed and calculated contrail cloud cover with respect to air traffic

Compared to the results for Europe for which the contrail frequency is derived by the same procedures (Mannstein *et al.* 1999) and by the same satellite instrument

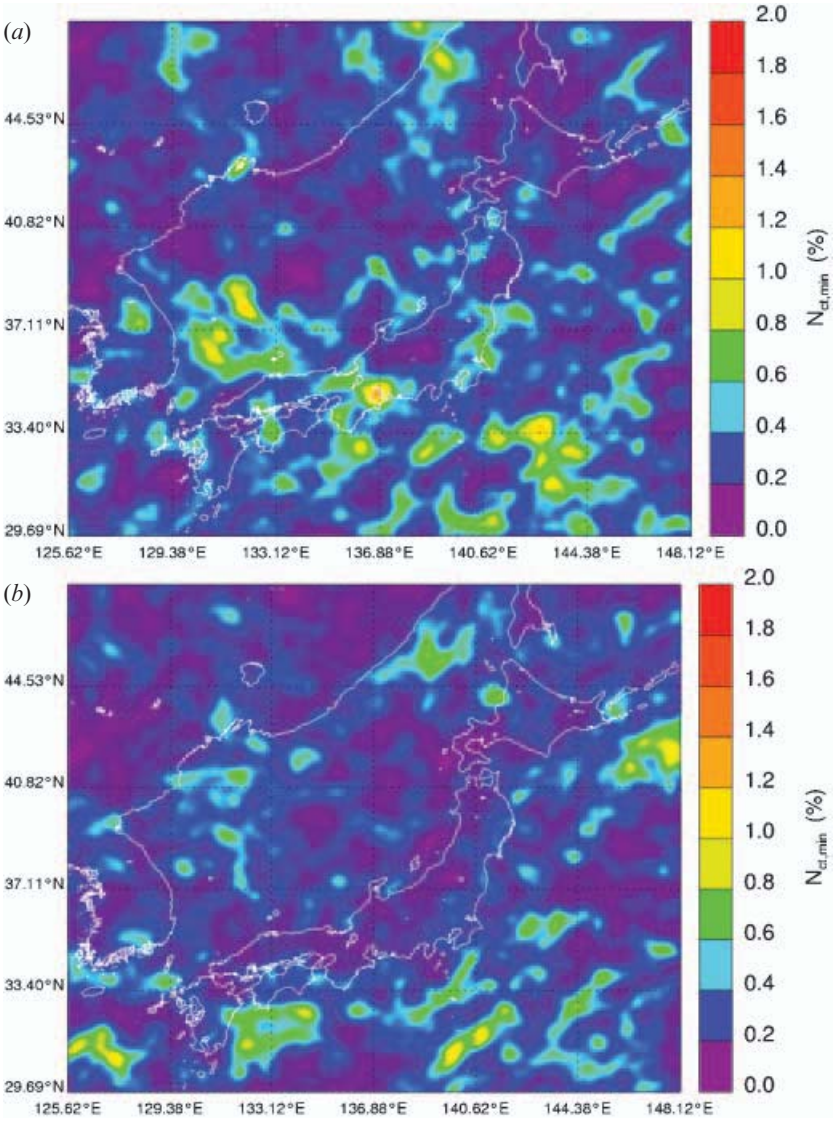

Figure 6. Japan region: Annual mean contrail coverage by line-shaped contrails (lower estimate) derived from AVHRR data of the year 1998 (average from 4 months of daily data). Map (*a*) displays daytime data (mean satellite overpass time 4:53 UT=13:53 Tokyo time), map (*b*) night time data (17:54 UT=2:54 Tokyo time). All displayed values are based on a minimum number of 16 measurements, which is essential to derive average values for the ECHAM4 boxes in T30 resolution (dashed lines). To get reliable results in the scale displayed in these maps a minimum of 64 measurements (see figure 2) are recommended.

(NOAA-14), contrail coverage is smaller for both Asian regions. Contrary to the results for Europe we observe almost the same amount of contrails during night than during day. How do these observational results fit to simulated contrail coverage and to actual air traffic emissions? In this section we compare the observations against model results derived by the climate model ECHAM4 and independent data on air traffic in the Asia/Pacific region.

4.1 *Simulation of contrails in the climate model ECHAM4*

Ponater *et al.* (2002) parameterised contrails in the comprehensive global circulation model (GCM) ECHAM4 (Roeckner *et al.* 1996). Contrails in this model are formed according to the modified Schmidt-Appleman-criterion (Schumann 1996) depending on the actual temperature and humidity in each model grid box at each time step. This leads to a fractional cloud cover that represents the maximum possible coverage, if air traffic in the box would be infinite. This potential contrail cover then is weighted linearly with the actual fuel consumption in the box. For this purpose, the DLR2 air traffic inventory for the year 1992 (Schmitt and Brunner 1997) is used, which includes the daily cycle of air traffic. Finally, to adapt the results to reality, the procedure is calibrated by use of observations of actual contrail cloudiness. As mentioned before, this study is based on the observations of Bakan *et al.* (1994). This study based on visual interpretations of AVHRR prints yields an average daytime contrail coverage of 0.5% for the region of Europe and the Eastern Atlantic which is marked in figure 1 and was used to calibrate the full-day averages of the contrail simulations in Ponater *et al.* (2002). However, for this region Bakan *et al.* (1994) find a day/night-ratio of two. Thus, the actual full-day average should be 0.375%. This value is used here for the new GCM study presented in the paper on hand. Thus, the simulated contrail coverage results given here are approximately 25% lower than the results of Ponater *et al.* (2002). Additionally, the new GCM run for the first time includes the daily cycle of air traffic based on the only presently available global 3D data set with a 2-hourly temporal resolution (Schmitt and Brunner 1997). As this emission data set provides only data for March 1992, we assume a consistent daily cycle throughout the year and use this as weighting factor for the monthly resolved air traffic data used by Ponater *et al.* (2002). The simulations run over five years for mean 1992 conditions. It enables to study the diurnal contrail cover changes and compare them to observations.

A second GCM run was done using a projection of the DLR2 air traffic inventory to the year 2015. For this purpose regionally different growth rates of air traffic according to Schmitt and Brunner (1997) are used. The climatological situation is assumed to be identical for 1992 and 2015.

4.2 *Comparison of AVHRR-observations and ECHAM4 results*

For Europe the results on contrail coverage derived from AVHRR data and given by Mannstein *et al.* (1999) are approximately 50% below the results of the GCM. This can be explained mainly by the underestimation of the observed contrail cover through neglecting widespread contrail features. How is the situation in the Asian regions far off the region which is used for the calibration of the GCM? Comparing the observed contrail coverage (figures 5 and 6) to the simulated contrail coverage (figure 7) it can be seen that the patterns of the regional distributions agree well. Quantitative results from the AVHRR-observations over Asia and from the model are given in table 1. To compare model results and observations the ratio of observed coverage against modelled coverage in 1992 is also included on table 1.

Surprisingly, for both Asian regions the observation to simulation ratio is opposite to the result for Europe: Especially for the Thailand region the observations are 74% higher than the model results. For the Japan region the difference is less (+46%), but there were also more contrails observed than the model created. From the seasonal separation of the data in table 1 can be seen that this

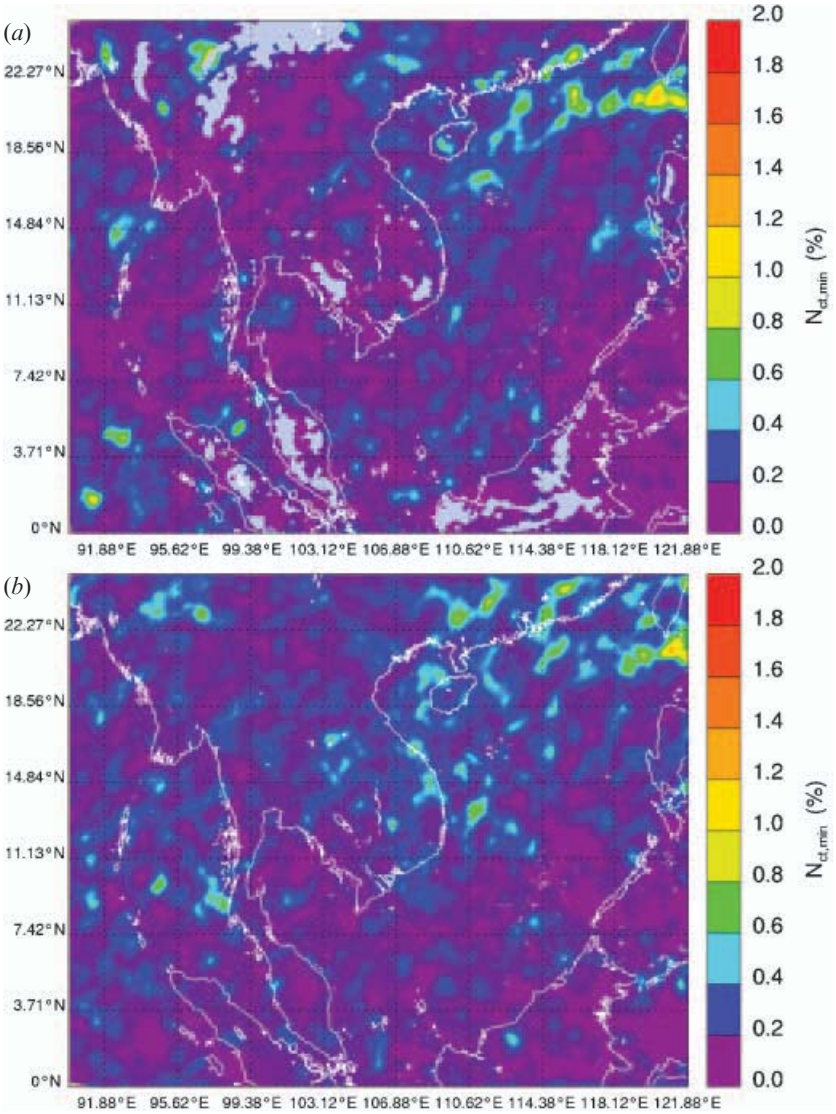

Figure 7. Thailand region: In this region during daytime at some places (grey regions in map (*a*)) the background heterogeneity *SDT5* exceeds 1.1 K. There, contrail detection is doubtful. Daytime (*a*) here is related to a mean satellite overpass time of 7:45 UT (14:50 Bangkok time) and 20:05 UT (3:05 Bangkok time) for night-time (*b*). See also the caption of figure 5 for additional description.

difference seems to be similar throughout the annual cycle. In both regions the observation/simulation-ratio is outlaying for the month of October. This could be a hint that contrail coverage derived from one month of data has low significance as it is possible to have untypical weather situations during a one month period. The annual averages calculated by the model are based on 12 months, and therefore can differ from a 4-months-average. Actually for the Japan region the 12-months-average is 14% higher than the 4-months-average for 1992 and 28% higher for 2015. This may be caused by neglecting April and May which show the highest contrail

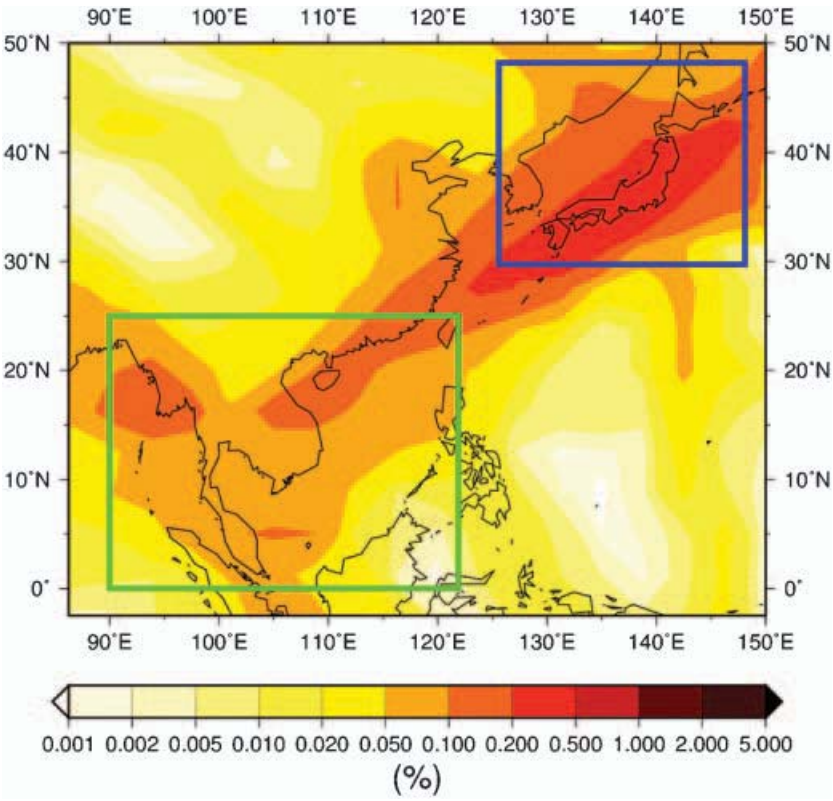

Figure 8. Annual daily mean contrail coverage as simulated by ECHAM4 related to aircraft emissions of 1992. Thailand region: green rectangle, Japan region: blue.

coverage in the model data. To give more significant results observations of all months best for several years preferably including the simulated year are needed.

One reason for the quantitative discrepancy between observation and the 1992 model studies may be the growth of air traffic in these regions between 1992 and

Table 1. Comparison of remote sensing observations on contrail cloud cover (seasonal and annual averages) in 1998 against ECHAM-modelled contrail cloud cover (reference year 1992 and projection to 2015). The annual averages are calculated from 4 months for the AVHRR observations and from 12 months for the model-derived values.

		Contrail coverage (%)			Ratio
		AVHRR	ECHAM	ECHAM	Obs./mod.
Region	Time period/ref. year	1998	1992	2015	1998 vs. 1992
Japan	January	0.15	0.11	0.30	1.4
	March	0.31	0.24	0.58	1.3
	July	0.26	0.17	0.54	1.6
	October	0.27	0.10	0.47	2.6
	Annual average	0.25	0.17	0.60	1.5
Thailand	January	0.18	0.07	0.24	2.8
	April	0.19	0.09	0.49	2.1
	July	0.08	0.04	0.11	2.2
	October	0.06	0.07	0.41	0.8
	Annual average	0.13	0.06	0.31	1.7

1998. This is supported by the significant increase in modelled contrail cover from 1992 to 2015 (see table 1), which amounts to a factor of 3.5 for the Japan region and about 5 for the Thailand region. If, as a first guess, linear increase in contrail cover between the two time slices is assumed, the expected cover from model data for 1998 comes very close to the observed values. Note also that the modelled contrail cover is likely to be underestimated in tropical regions (i.e. large parts of the Thailand region) due to systematic errors on the ECHAM4 model climate (F. Mager, personal communication).

A comparatively strong growth of air traffic especially in Southeast Asia is also mentioned from IPCC (1999). Furthermore the strong political changes in the beginning of the 1990s could have allowed completely different routing in the late 1990s. Changes in air traffic in this region are also reported by ATAG (1997). During the period from 1990 to 1996 the annual growth rate in the route sectors relevant to the regions of our study were in the range from 9% (Tokyo FIR (flight information region)) to 15% (South China Sea). The best estimate is 11% which is much higher than e.g. the growth rate in the North Atlantic flight corridor. There, according to IATA (1994) it was only about 6%. Thus, air traffic in the Asian regions investigated here should almost have doubled (+85%) during the six years from 1990 to 1996. As the time difference from our 1998 contrail observations to the 1992 related ECHAM4 simulations is the same, it is realistic to assume a doubling of the air traffic in between. This strong growth can explain some of the relatively high observational values indicated in the prior subsection. From the 6% growth rate for Europe and the smaller time difference of only 4 years – Mannstein *et al.* (1999) observed the year 1996 – a total growth of +22% against 1992 is assumed.

Another interesting comparison between observations and models can be made analysing daytime versus night time contrail coverage. For this purpose the ECHAM-derived contrail coverage was calculated for the AVHRR-appropriate time slices. Through temporal weighting of three or four 2-h time slices it was possible to represent closest the time period that is observed by AVHRR. The results of this comparison are given in table 2. In §3.3 (figures 5 and 6) it was already stated that the observed contrail coverage during day and night was approximately equal for both Asian regions. For the Thailand region the day/night-ratios of observation and model agree perfectly. However, large differences occur when we make the same comparison for the Japan region. What could be the reason for the much stronger contrail formation during night-time in the year 1998?

Perhaps a part of the large day/night-ratio observed for the Japan region may also be explained by a change in the air traffic diurnal cycle between 1992 and 1998.

Table 2. Comparing annual mean contrail cloud cover for different times of day. AVHRR observations, ECHAM-modelled contrail results and flights from ATAG.

		AVHRR	ECHAM	ATAG
	Reference year	1998	1992	1996
Region	Time period	Contrail coverage (%)		Flights/hour
Japan	Day	0.27	0.30	44
	Night	0.22	0.03	10
	Day/night ratio	1.2	9.2	4.4
Thailand	Day	0.12	0.07	42
	Night	0.14	0.08	31
	Day/night ratio	0.9	0.9	1.4

ATAG (1997) reports air traffic frequency on a hourly basis for the year 1996. Separation into six different route sectors in the Asia/Pacific air traffic region helps to develop a differentiated view on the day/night-ratios of both regions. For this purpose a route-number weighted hourly average of the flights for both regions was calculated. These hourly values then are convoluted with a temporal filter similar to the temporal weighting of the ECHAM4 results. The results in flights per hour therefore should be closely correlated to the AVHRR overpass periods. Additionally these numbers are indicated in table 2. Again the day/night-ratio fits quite well for the Thailand region. For the Japan region the ATAG-ratio related to 1996 is in between observations related to 1998 and simulations related to 1992. Air traffic growth there seems to be vary according to the various daytimes. These numbers make the observed high values for night time contrail cover in the Japan region plausible.

5. Discussion of contrail coverage over Southern and Eastern Asia

The weather of the Japan region is dominated by mid latitudinal and subtropical characteristics. Contrail formation there should follow the characteristics known from Europe which are described e.g. by Kästner *et al.* (1999). Analysing the monthly mean contrail cover (table 1) a distinct seasonal variability can be noticed. In spring for both Asian regions the highest contrail cover is derived from satellite data and from simulations. This is also in agreement with Chen *et al.* (2001), who show that the most favourable seasons for contrail formation above Taiwan are winter and spring. During the months July and October the smallest contrail cover is observed in the AVHRR data.

The meteorological situation in the mostly tropical Thailand region is very different from mid-latitudes. The most important sources for water vapour in the free atmosphere are the detrainment of saturated air from deep cloud tops, the evaporation of hydrometeors which are pumped into the upper atmosphere by deep convection and the evaporation of precipitation generated by upper level clouds (Sun and Lindzen 1996). Deep convection induces large-scale subsidence which leads to nearly adiabatic heating and therefore to a decrease of relative humidity (RH) in the subsiding air (Sun and Lindzen 1996). This may cause dissipation of contrails. In addition, RH decreases from 44–47% nearby the cloud top edges to 11–15% at a distance of about 500 km from the cloud centre. The diurnal cycle of humidity in the upper troposphere has a time lag of approximately 8 hours beyond the diurnal cycle of convection (Udelhofen and Hartmann 1995). Thus, at noon and in the afternoon, suitable atmospheric conditions for contrail formation should only be found in the close neighbourhood of deep convective systems. These regions are normally smaller than the warm conveyor belt of a warm front, or the fast rising air in front of a cold front, which are suitable regions for contrail formation in midlatitudes (Kästner *et al.* 1999). This could be a reason for the relatively high frequency of observed contrails in the tropics. RH is somewhat lower at the cloud edges of deep convection over land than over sea. Also the total number of deep convective systems over land is smaller than over sea (Udelhofen and Hartmann 1995). Therefore, there should be a higher frequency of suitable conditions for contrail formation over land surfaces.

As given in table 2 the small observed diurnal variance of contrails (day/night-factor of 0.9) in the Thailand region fits very well to the ECHAM-derived day/night-ratio, but it does not follow the diurnal variance of air traffic (approximately a day/

night-factor of 1.4). An explanation could be the typical meteorological situation in the tropics. The mean overpass time of the NOAA-14 satellite in the Thailand region for noon is around 14:50 local time. This is close to the maximum of deep convection (Asnani 1993). Thus, formation of persistent contrails is probably reduced by the reasons mention above. At night no deep convection occurs. On the other hand, now RH is relatively high in the upper atmosphere. Therefore the conditions for the formation of persistent contrails are more suitable at night than at day.

6. Conclusions

This paper for the first time reports on systematic satellite observations of contrails over Asia. The AVHRR-observed contrail cover in both regions was higher than expected from the extrapolation of the European contrail coverage obtained from GCM simulations in ECHAM4. One reason may be the extraordinarily high growth rates of air traffic and the six year time lag from the emission data used for the GCM simulation and the AVHRR observations.

The annual cycle of contrail coverage is sampled by four months of twice daily AVHRR-data. Strong seasonal effects are observed with a peak during spring for both regions. The Japan region shows its minimum during winter while the Thailand region has the minimum during autumn. The model-derived contrail coverage, which is available for 12 climatological months based on five years, follows these seasonal characteristics. For the Japan region the maximal values of the model-derived contrail coverage are found in April and May. These extreme values are missed by the selected observations and one month of a single year is also not highly significant. Thus, we conclude that more observational data are necessary – at least 12 months from two years – to get a more detailed view on seasonal characteristics.

The small diurnal cycle of contrail coverage observed in the Thailand region can be conclusively explained by meteorological reasons (strong convection during daytime and high humidity during night). However, the same arguments can only be partly applied to the Japan region. They cannot sufficiently explain the large differences between observed and modelled day/night-ratios (observations: 1.2 versus model: 9.2). It is likely that major changes in the daily air traffic patterns happened in the six year time span between 1992 (reference year for the emission data set) and 1998 (observations).

Variations of the observed coverage mostly have a scale in the range of 50 km to 100 km (Meyer *et al.* 2002). This is much smaller than the ECHAM4 T30 grid size in the order of 400 km. Therefore, the satellite data show much stronger variations with higher extreme values. To allow a more detailed analysis in the future there is an explicit need for flight emission inventories with a good horizontal resolution of at least 100 km. An hourly temporal resolution will greatly improve the possibilities for future comparisons and will allow much more realistic simulations.

The comparison between the GCM calculated and observed contrail data is very promising. It shows where interesting open questions in the field of contrail research can be found, e.g. improved parameterization in the model or validation of the remote sensing techniques. A global assessment of contrail observations against model data can greatly improve our knowledge and understanding of contrail effects on climate. One of the most important questions remaining open is how much of the observed line-shaped contrails are converted into contrail–cirrus which may cover much larger areas.

Acknowledgements

This work was partly funded by the European Commission within the Project CLOUDMAP (EU contract no. ENV4 CT97-0399). We thank Michael Ponater from DLR for the fruitful discussion of the ECHAM model results and Toshiro Nemoto from the University of Tokyo and the Asian Institute for Technology, Bangkok for providing the NOAA/AVHRR data.

References

ASNANI, G.C., 1993, *Tropical meteorology*, Vol. 1 (Pune, India: Noble Printers).

ATAG, 1997, Asia/Pacific air traffic growth & constraints. Air Transport Action Group, Geneva, Switzerland, http://www.atag.org/ASIA/Index.htm.

BAKAN, S., BETANCOR, M., GAYLER, V. and GRASSL, H., 1994, Contrail frequency over Europe from NOAA-satellite images. *Annales Geophysicae*, **12**, pp. 962–968.

CHEN, J.-P., LIN, W.-H. and LIN, R.-F., 2001, Estimation of contrail frequency and radiative effects over Taiwan area, Terrestrial. *Atmospheric and Oceanic Sciences*, **12**, pp. 155–178.

GIERENS, K., SAUSEN, R. and SCHUMANN, U., 1998, A diagnostic study of the global coverage by contrails, Part II: Future air traffic scenarios. *Theoretical and Applied Climatology*, **63**, pp. 1–9.

IATA, 1994, North American traffic forecasts 1980–2010, International Air Transport Association Publications Assistants, Geneva, Switzerland.

IPCC, 1999, Aviation and the global atmosphere. Edited by J.E. Penner, D.H. Lister, D.J. Griggs, D.J. Dokken and M. McFarland, *Intergovernmental Panel on Climate Change* (Cambridge: Cambridge University Press).

JENSEN, E.J., TOON, O.B., KINNE, S., SACHSE, G.W., ANDERSON, B.E., CHAN, K.R., TWOHMY, C.H., GANDRUD, B., HEYMSFIELD, A. and MIKAE-LYE, R.C., 1998, Environmental conditions required for contrail formation and persistence. *Journal of Geophysical Research*, **103**, pp. 3929–3936.

KÄSTNER, M., MEYER, R.C.C. and WENDLING, P., 1999, Influence of weather conditions on the distribution of persistent contrails. *Meteorological Applications*, **6**, pp. 261–271.

LIOU, K.N., OU, C.C. and KOENIG, G., 1990, An investigation of the climatic effect of contrail cirrus. In *Air Traffic and the Environment: Background, Tendencies, and Potential Global Atmospheric Effects*, edited by U. Schumann (Berlin: Springer-Verlag), pp. 154–169.

MANNSTEIN, H., MEYER, R. and WENDLING, P., 1999, Operational detection of contrails from NOAA-AVHRR-data. *International Journal of Remote Sensing*, **20**, pp. 1641–1660.

MARQUART, S. and MAYER, B., 2002, Towards a reliable GCM estimation of contrail radiative forcing. *Geophysical Research Letters*, **29**, pp. 1–4.

MEYER, R., MANNSTEIN, H., MEERKÖTTER, R., SCHUMANN, U. and WENDLING, P., 2002, Regional radiative forcing by line-shaped contrails derived from satellite data. *Journal of Geophysical Research*, **107**, pp. 1–16.

MINNIS, P., SCHUMANN, U., DOELLING, D.R., GIERENS, K.M. and FAHEY, D.W., 1999, Global distribution of contrail radiative forcing. *Geophysical Research Letters*, **26**, pp. 1853–1856.

PONATER, M., BRINKOP, S., SAUSEN, R. and SCHUMANN, U., 1996, Simulating the global atmospheric response to aircraft water vapour emissions and contrails: A first approach using a GCM. *Annales Geophysicae*, **14**, pp. 941–960.

PONATER, M., MARQUART, S. and SAUSEN, R., 2002, Contrails in a comprehensive climate model: Parameterisation and radiative forcing. *Journal of Geophysical Research*, **107**, pp. D13, ACL 2–1–10.

ROECKNER, E.K., ARPE, L., BEGTSSON, M., CHRISTOPH, M., CLAUSSEN, M., DÜMENIL, L., ESCH, M., GIORGETTA, M., SCHLESE, U. and SCHULZWEIDA, U., 1996, The

atmospheric general circulation model ECHAM-4: Model description and simulation present day climate. Rep. 218, Max-Planck-Institut für Meteorologie, Hamburg, Germany.

SAUSEN, R., GIERENS, K., PONATER, M. and SCHUMANN, U., 1998, A diagnostic study of the global distribution of contrails. Part I: Present day climate. *Theoretical and Applied Climatology*, **61**, pp. 127–141.

SCHMITT, A. and BRUNNER, B., 1997, Emissions from aviation and their development over time. In Pollutants from Air Traffic – Results of Atmospheric Research 1992–1997, DLR-Forschungsbericht 97–04, Deutsches Zentrum für Luft- und Raumfahrt, Köln, Germany, pp. 37–52.

SCHUMANN, U., 1996, On conditions for contrail formation from aircraft exhausts. *Meteorologische Zeitschrift*, **5**, pp. 4–23.

SCHUMANN, U., 2002, Contrail cirrus. In *Cirrus*, ed. D. Lynch, K. Sassen, D.O. Starr and G. Stephens (Oxford: Oxford University Press), pp. 231–255.

STRAUSS, B., MEERKÖTTER, R., WISSINGER, B., WENDLING, P. and HESS, M., 1997, On the regional climatic impact of contrails: Microphysical and radiative properties of contrails and natural cirrus clouds. *Annales Geophysicae*, **15**, pp. 1457–1467.

SUN, D.Z. and LINDZEN, R.S., 1996, Distribution of tropical tropospheric water vapor. *Bulletin of the American Meteorological Society*, **50**, pp. 1643–1660.

UDELHOFEN, P.M. and HARTMAN, D., 1995, Influence of tropical cloud systems on the relative humidity in the upper troposphere. *Journal of Geophysical Research*, **100**, pp. 7423–7440.